Assessing progressive mechanical instability of submarine slopes caused by methane hydrate dissociation

Jiangzhi Chen[1] and **Shenghua Mei**[1] and **Dawei Wang**[1] and **Jin Sun**[1] and **Yue Sun**[1]

[1]Institute of Deep-Sea Science and Engineering, Chinese Academy of Sciences

Key Points:

- Gas hydrates on continental slopes may trigger submarine landslides, which poses a major threat for offshore infrastructures.
- Conventional infinite slope analysis neglects finite rupture that might progressively escalate to catastrophic landslides.
- Numerical model integrating slip nucleation and gas hydrate dissociation is developed to link gas hydrate dissociation and landslides.
- Progressive failure can be induced by minor changes in gas hydrates, influenced by failure surface depth and sediment characteristics.

Corresponding author: Dawei Wang, `wangdawei@idsse.ac.cn`

Abstract

Large amounts of gas hydrates exist on continental slopes, and pose a significant risk of triggering submarine landslides, subsequently impacting offshore infrastructures. While the infinite slope model is widely used for submarine slope stability analysis, it overlooks the potential for initial small failures to develop into large landslides. Our study integrates slip nucleation with excess pore pressure during gas hydrate dissociation, establishing a model for progressive slope failure triggered by hydrate dissociation. Focusing on the Shenhu hydrate site GMGS3-W19, our results show that even 1% gas hydrate dissociation contributing to about 1 MPa overpressure can induce progressive landslides. Notably, deeper failure surfaces with gentler slopes and collapsible sediments require higher pore pressures to induce progressive failure, reducing the risk of developing into catastrophic landslides. The results indicate that the infinite slope model may overestimate slope stability, and that submarine landslides caused by progressive failure may occur on slopes previously considered stable, such as the Ursa Basin in the northern Gulf of Mexico. This extension of the infinite slope model sheds light on potential limitations in current stability assessments, providing crucial insights for submarine landslide studies and offshore infrastructure development.

Plain Language Summary

Understanding the stability of submarine slopes is crucial for assessing the risks associated with submarine landslides, particularly for safeguarding offshore structures. However, commonly used models, like the infinite slope model, often overlook the potential for small initial failures to escalate into larger, more significant collapses over time. This study introduces an innovative approach by integrating different models to explore how changes in gas hydrate conditions might influence slope stability. Our investigation focused on Shenhu Site GMGS3-W19 revealed a surprising observation: even minor alterations in gas hydrate conditions can trigger substantial landslides. Furthermore, our findings suggest that with softer underlying materials at greater depths below seafloor, buried slopes require higher pressures to reach failure.

This research highlights a notable limitation in current slope stability models: their tendency to underestimate slope vulnerability, disregarding the possibility of substantial landslides for regions such as the Ursa Basin. By identifying these limitations, our study aims to provide valuable insights for researchers and engineers involved in submarine landslide studies and offshore infrastructure development. In summary, our novel approach to assessing slope stability prompts a reevaluation of conventional methods, potentially enhancing the accuracy of assessing submarine slope safety and bolstering the resilience of offshore installations.

1 Introduction

Gas hydrates are ice-like crystals in which guest molecules such as methane or carbon dioxide are trapped in cages formed by water molecules. These hydrates remain stable under low-temperature and high-pressure conditions, and are mainly stored in permafrost on land or in marine sediments (Ginsburg et al., 1995). The amount of methane hydrate stored in marine sediments is estimated to be $\sim10^4$ Gt (Kvenvolden, 1988), and has attracted increasing attention as a possible energy source. Submarine methane hydrate deposits exist mainly on the continental slope in the hydrate stability zone, a region defined by the hydrate-gas phase boundary and the bulk geothermal temperature profile (Kvenvolden, 1988; Sloan & Koh, 2007), and the base of the hydrate stability zone (BHSZ) in the bulk state is uniquely determined by the three-phase equilibrium of the hydrate phase, free gas phase and dissolved methane phases, depending on the temperature, pressure, and salinity. Despite being a promising energy source, methane hydrate is also a submarine geohazard that threatens offshore infrastructure, including platforms,

66 pipelines, and power and telecommunications cables, because natural or anthropogenic
67 perturbations in the temperature and the pressure can cause the hydrate to dissociate,
68 alter the stability of sediments, and lead to gas escape, sediment collapse, or even land-
69 slides on the continental slope (Maslin et al., 2010).

70   Among the factors that can contribute to submarine landslides, such as earthquakes,
71 sea-level change (e.g., Lafuerza et al., 2012; Berndt et al., 2012; Riboulot et al., 2013;
72 Smith et al., 2013; Brothers et al., 2013) or iceberg collision (Normandeau et al., 2021),
73 gas hydrate dissociation poses a more imminent risk because gas hydrates are ubiqui-
74 tous in the marine sediments, and the dissociation can be triggered by small perturba-
75 tions in the temperature and the pressure. For example, the Storegga Slide on the Nor-
76 wegian continental shelf, one of the largest known submarine landslides, is widely believed
77 to have been triggered by hydrate dissociation (Sultan et al., 2004; Brown et al., 2006).
78 Mechanically, the instability of the continental slope can be caused by an increase in the
79 shear stress of the overlying layer or by a decrease in the strength of the slope. Since the
80 weight of the overburden, the frictional properties, and the sediment cohesion remain rel-
81 atively unchanged in the short term, the stability of the slope is primarily determined
82 by the elevated pore pressure during the hydrate dissociation.

83   Submarine landslides on continental slopes are considered to occur on a rupture
84 surface with a depth much smaller than its length, and infinite slope analysis is typically
85 invoked to assess the slope stability. For gas hydrate-related landslides, the stability at
86 the potential slip surface (usually assumed to be the BHSZ) is assessed using the safety
87 factor F_S, i.e., the ratio of the frictional resistance at the slip surface to the shear stress
88 of the overlying layer (e.g., Kayen & Lee, 1991; Sultan et al., 2004; Nixon & Grozic, 2007).
89 Although the infinite slope model is widely used, the validity of the safety factor relies
90 on some simplified assumptions. The model assumes that the BHSZ is where the slip starts,
91 and that hydrate dissociation occurs simultaneously over the entire potential slip sur-
92 face. The entire slope is assumed to have homogeneous sediment and frictional proper-
93 ties. Some researchers have attempted to relax the assumptions by allowing the slip sur-
94 face not to coincide with the BHSZ (e.g., Sultan et al., 2004), but these models still as-
95 sume homogeneous frictional properties. Most importantly, the infinite slope model and
96 its modified versions, however, neglect the possibility that hydrate may dissociate at cer-
97 tain small finite region on the surface, and then the slip nucleates and progressively de-
98 velops into a large-scale catastrophic landslide.

99   In this study, we combine the excess pore pressure with the slip nucleation model
100 by Viesca and Rice (2012) and develop a model of progressive slope failure caused by
101 hydrate dissociation. The landslide is initiated on a finite length patch with slip-weakening
102 friction. The result can be used to extend the slope stability analysis with a convenient
103 corrector for progressive submarine landslide risk assessment.

2 Initiation of progressive failure

105   First we review the infinite slope model and then present the theoretical framework
106 for simulating the triggering of progressive slope failure, where the slip at the finite patch
107 reduces the friction and changes the shear stress.

2.1 Infinite slope analysis

109   If the sediment porosity is ϕ, the saturated unit weight of the soil is $\gamma = \rho_s(1 -
110 \phi)g + \rho_l \phi g$, the unit weight of the water is $\gamma_l = \rho_l g$, and the submerged unit weight of
111 the soil is $\gamma' = \gamma - \gamma_l$. On the sliding interface with a dip angle β, the shear stress is
112 the destabilizing gravity component along the slope $\tau_0 = \gamma'(H + D)\sin\beta\cos\beta$ where
113 H is the depth below the seafloor to the hydrate layer of a thickness D, and γ' is the sub-
114 merged unit weight of the overlying layer. The failure surface is assumed to locate at the

base of the hydrate layer (Figure 1). The shear stress is balanced by the frictional re-
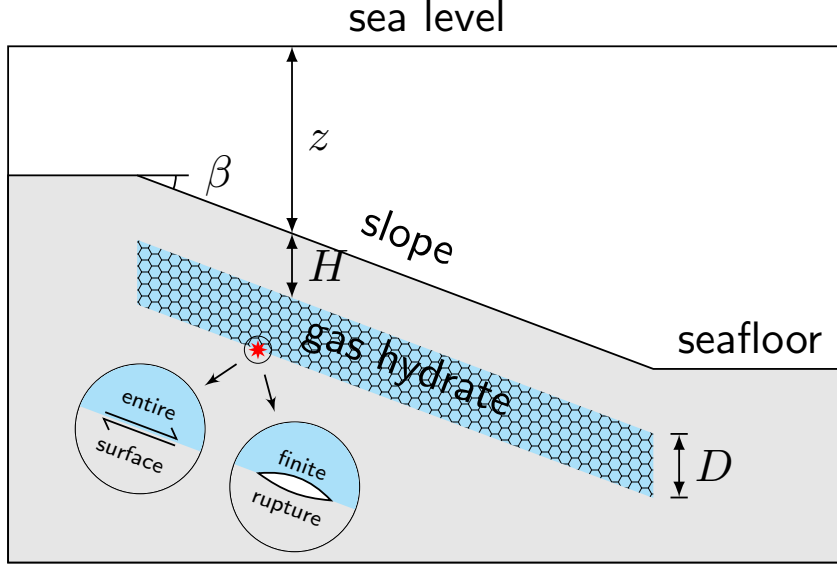

Figure 1. A schematic of the hydrate-bearing sediments on a submarine slope. The failure (labeled with a red star) occurs at the base of the hydrate layer of a thickness D, with an overlying sediment layer of a thickness H. The failure may be along the entire BHSZ, or start with a small rupture of a finite size.

sistance

$$\tau_0 \leq c + f\left(\sigma_0 - \Delta u\right) \tag{1}$$

where c is the cohesion, f is the friction coefficient, $\sigma_0 = \gamma'(H + D)\cos^2\beta$ is the normal stress, and Δu is the excess pore pressure. With the entire failure surface sliding and the friction is taken as constant static friction $\tan\psi$ where ψ is the friction angle, the safety factor is defined as (Duncan et al., 2014)

$$F_S = \frac{c + \tan\psi\left(\sigma_0 - \Delta u\right)}{\tau_0} = \frac{c + \tan\psi\left[\gamma'(H+D)\cos^2\beta - \Delta u\right]}{\gamma'(H+D)\sin\beta\cos\beta}. \tag{2}$$

For unconsolidated sandy sediments, c is usually close to zero, and cementation caused by hydrates is neglected at low to moderate hydrate saturation. The hydrate in the pore spaces is assumed to have neutral buoyancy because the hydrate density is close to the pore water density. When $F_S > 1$ the resisting forces are greater than the destabilizing forces, and the slope is considered stable. A slope is critically stable when $F_S = 1$, but in practice the threshold of F_S is often taken to be slightly larger than unity (1.2 or 1.5). The value F_S does not explicitly depend on the water depth because the contribution of water weight in the overburden is canceled out by the hydrostatic pore pressure.

The infinite slope analysis is typically employed in conventional slope failure assessment due to its simplicity. However, if the failure first occurs on a finite patch, the opening of the finite patch induces an additional term on the shear stress and alters the force balance.

2.2 Slip nucleation on a finite patch

The difference between the infinite slope model and the finite patch model is that the former assumes that the slip occurs on the entire BHSZ, while the latter assumes that the slip occurs on a finite patch. When a finite patch of a length $2a$ at a sliding surface far away from a free surface is set to slip, for cohesionless scenario the stress balance becomes (Viesca & Rice, 2012)

$$f\left[\sigma_0 - \Delta u(x,t)\right] = \tau_0 - \frac{G}{2\pi(1-\nu)} \int_{-a}^{a} \frac{\partial\delta/\partial\xi \,\mathrm{d}\xi}{x-\xi} \qquad (3)$$

where σ_0 and τ_0 are the same normal and shear stress caused by the effective weight of the layer, $\delta(x,t)$ is the slip distance on the patch, G is the shear modulus and ν is the Poisson ratio. Without the stress caused by the rupture, the cohesionless infinite slope model is recovered. Equation (3) describes how the stress state on the potential sliding surface is perturbed beyond the initial failed patch, and can be reduced to an eigenvalue problem for $V = \mathrm{d}\delta/\mathrm{d}t$ if we take into account the weakening of the frictional resistance with δ (Viesca & Rice, 2012) with a linear slip-weakening law

$$f(\delta) = \tan\psi - \delta\Delta f/D_c \qquad (4)$$

where $\Delta f = \tan\psi - f_{\mathrm{ss}}$ is the friction drop between the maximum static friction $\tan\psi$ and the steady-state friction f_{ss}, and D_c is a characteristic length of the slip, typically on the order of millimeters or centimeters as suggested by rock experiments (Rice & Ruina, 1983; Marone, 1998). The eigenvalue problem gives a solution of the critical excess pore pressure

$$\Delta u_{\mathrm{slip}} = \sigma_0 - \frac{\lambda_0 D_c G}{\Delta f a(1-\nu)} \qquad (5)$$

where $\lambda_0 \approx 0.579$ is the smallest eigenvalue. Detailed description can be found in Viesca and Rice (2012), and a brief derivation is provided in Appendix A.

The critical excess pore pressure Δu_{slip} required for slip nucleation depends on the normal stress σ_0, the shear modulus G, the characteristic length D_c, the patch size a, and the friction drop Δf. Since for submarine landslides the steady-state friction coefficient is $f_{\mathrm{ss}} \ll \tan\psi$, the friction drop is $\Delta f \approx \tan\psi$, and the scaled crack size $\chi = a/D_c$ determines the critical excess pore pressure. The slip starts with a small slip with respect to D_c, which is in the order of millimeters, and the minimal value of χ is determined by setting Δu_{slip} to zero

$$\chi_{\mathrm{min}} = \frac{G\lambda_0}{\sigma_0\Delta f(1-\nu)}. \qquad (6)$$

For a typical submarine slope with the slip located at a depth of $\sim 100\,\mathrm{m}$ below seafloor, the shear modulus is $G/(1-\nu) \sim 100\,\mathrm{MPa}$, the normal stress $\sigma_0 \sim 1\,\mathrm{MPa}$, and the value $\chi_{\mathrm{min}} \sim 10^2$. The values of a and D_c are neither well constrained, but only their ratio χ appears in the results which is of the same order of magnitude as χ_{min}, so we incorporate their uncertainties in χ. The critical excess pore pressure Δu_{slip} can thus be expressed as

$$\Delta u_{\mathrm{slip}} = \sigma_0(1 - \chi_{\mathrm{min}}/\chi). \qquad (7)$$

It is clear that progressive failure may initiate when the safety factor F_S is still greater than unity.

2.3 Overpressure caused by hydrate dissociation

Extensive studies exist to estimate the increase in pore pressure when the methane hydrate dissociates (e.g., Xu & Germanovich, 2006; Kwon et al., 2008; Lee et al., 2010). We follow the theoretical model developed by Xu and Germanovich (2006) to estimate

the overpressure. The excess pore pressure Δu from hydrate dissociation is related to the hydrate dissociation rate as

$$-\frac{R_v}{\kappa}\frac{\mathrm{d}S_h}{\mathrm{d}t} = \frac{\Delta u}{t_d} + \frac{\mathrm{d}\Delta u}{\mathrm{d}t} \tag{8}$$

where t is the time, R_v is the volume expansion factor depending on the saturation levels of the liquid and gas phases (see Appendix B1 for details), S_h is the hydrate saturation with an initial value S_h^0, κ is the compressibility of the gas, hydrate, and liquid solution at the three-phase equilibrium (Appendix B2), and $t_d = \kappa\mu\phi DH/k$ is the characteristic dissipation timescale determined by the effective permeability k, the viscosity of the pore water μ, the thickness of the dissociating hydrate layer D, and the depth of the layer to the seafloor H. Note that κ is a function of S_h and the pore pressure P, which depends on both the overburden and compression caused by previously dissociated hydrate.

For a typical submarine hydrate reservoir, $\kappa \sim 1\,\mathrm{GPa}^{-1}$, $\mu \sim 10^{-3}\,\mathrm{Pa\cdot s}$, $DH \sim 10^4\,\mathrm{m}^2$, $k \sim 10^{-15}\,\mathrm{m}^2$, so $t_d \sim 10^7\,\mathrm{s} \approx 0.3\,\mathrm{yr}$. A typical landslide occurs at a timescale $t \ll t_d$, in contrast with a slow sliding event which may last over a timescale much longer than t_d, so the hydrate dissociates instantaneously and the flux out of the pores can be ignored, which gives

$$\Delta u = -R_v \int_{S_h^0}^{S_h} \frac{\mathrm{d}S_h}{\kappa} \approx -\frac{R_v \Delta S_h}{\kappa(S_h^0)}. \tag{9}$$

where the approximation holds when $\Delta S_h = S_h^0 - S_h \ll S_h^0$ and κ barely changes, so the excess pore pressure is proportional to the amount of hydrate dissociated. Figure 2 shows how Δu varies with P and ΔS_h. For $\Delta u \leq 1\,\mathrm{MPa}$, the approximation is in good agreement with Δu for a wide range of P, and we will use this approximation in the following analysis.

3 Applications to real submarine slopes

From eq. (5) we can calculate the excess pore pressure threshold for the cascading failure to occur on a submarine slope, and eq. (9) gives the amount of hydrate required to dissociate if the overpressure is caused by hydrate dissociation. To demonstrate the difference between the infinite slope model and the progressive failure model, we first apply the model to a hydrate site in the Shenhu region, Northern South China Sea, to quantify the stability given the geological parameters, and next we use the model to explain the apparent high safety factors of the sites with landslides in the Ursa Basin, Northern Gulf of Mexico. The python scripts (Chen et al., 2023) are open-sourced under MIT license.

3.1 Shenhu Site GMGS3-W19, Northern South China Sea

Submarine landslides prevail in the continental slopes of the South China Sea from Miocene to present times (Wang et al., 2018). The gas hydrate-bearing sediments at Site GMGS3-W19, located in the Shenhu area in the Northern South China Sea, was studied in the third Chinese expedition in 2015. The parameters used in the model are listed in Table 1. Among these parameters, the thickness of the hydrate layer D and the Poisson's ratio ν are poorly constrained, and we use values of D and ν within the inferred range to calculate the critical values of Δu_{slip} and corresponding hydrate dissociation amount ΔS_h. The dissipation timescale is $t_d \approx 50\,\mathrm{d}$, so for most landslides occurring during a time period of a few days the instantaneous approximation eq. (9) can be used. We choose a scaled patch size $\chi = 100$, and calculate three representative slope dip angle values $\beta = 5°$, $10°$ and $15°$. Clearly, variations in χ play an important role in determining the slope stability to progressive failure, and we will return to the effects of variations in the Discussion section 4.1.
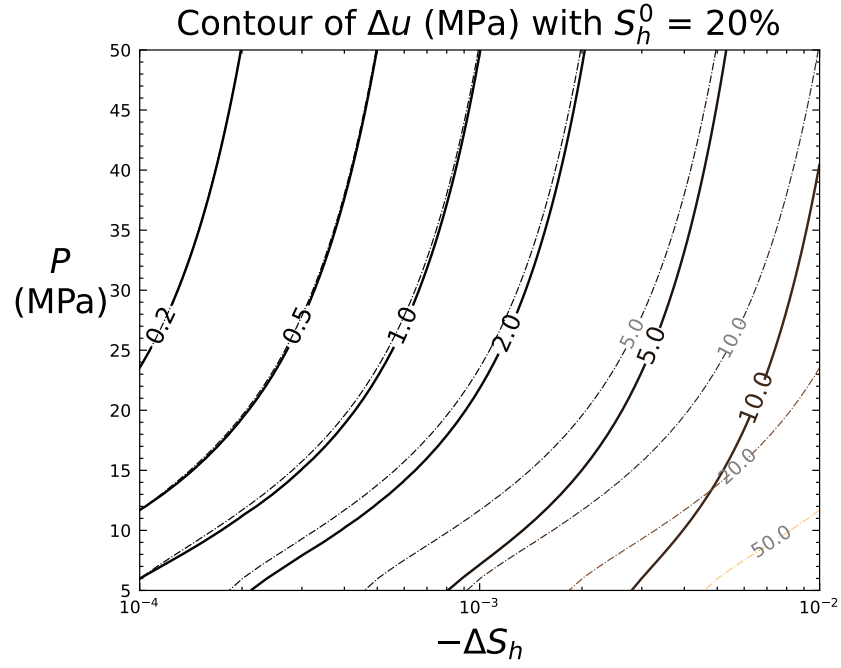
Figure 2. Excess pore pressure Δu caused by dissociation of hydrates with initial $S_h^0 = 20\%$ in a confined initially gas-free pore following Xu and Germanovich (2006). The solid contour lines are calculated using the integration, whereas the dashed contour shows the approximation of the small dissociation, with gray Δu values labeling the levels with significant deviations. Clearly, the approximation matches the Δu well for $\Delta u \leq 1\,\mathrm{MPa}$ for a wide pressure range.

Table 1. Model parameters for the Shenhu hydrate site.

	Parameter	Symbol	Unit	Value
	hydrate density [a]	ρ_h	kg/m^3	929
	seawater density [b]	ρ_l	kg/m^3	1029
physical parameters	dry sediment density	ρ_s	kg/m^3	2650
	molar mass of methane	M	g/mol	16.042
	methane mass fraction in hydrate	x	—	0.13
	water viscosity [c]	μ	Pa·s	
	water depth [d]	z	m	1273.8
	hydrate layer depth [d]	H	m	137.95
	maximum hydrate layer thickness [d]	D	m	17.6
	sediment porosity [d]	ϕ	—	0.483
	intrinsic sediment permeability [d]	k_0	m^2	5.5×10^{-15}
	initial hydrate saturation [d]	S_h^0	—	0.452
geological parameters	initial gas saturation [d]	S_g^0	—	0.194
	slope dip angle	β	°	
	friction angle [d]	ψ	°	25
	steady-state friction	f_{ss}	—	≈ 0
	Young's modulus [d]	E	MPa	70
	shear modulus [d]	G	MPa	$E/2(1+\nu)$
	Poisson's ratio [d]	ν	—	$0.15-0.45$

Sources: [a] Koh et al. (2011) [b] Spivey et al. (2004) [c] Straus and Schubert (1977)
[d] Sun et al. (2017)

Figure 3 shows how Δu_{slip} and F_S vary with different D, ν and β, and the corresponding amount of hydrate dissociated to attain Δu_{slip}. In Figure 3a, Δu_{slip} increases with thicker D, smaller β, and smaller ν. Mechanically, this indicates that if the BHSZ is deeper below the seafloor with a gentler slope and sediments easier to collapse, the risk of landslides is smaller. For the parameter ranges of interest, the excess pore pressure needed to initiate progressive failure is less than the critical pore pressure in the infinite slope model, indicated by the corresponding safety factor as high as 2.4 (Figure 3b). Therefore, the infinite slope model may overestimate the stability of the slope, and submarine landslides caused by progressive failure may occur on slopes that are previously considered stable. Because $\Delta u_{\mathrm{slip}} \lesssim 1\,\mathrm{MPa}$, the corresponding amount of hydrate dissociated can be readily estimated using eq. (9), and the result is shown in Figure 3c with a similar trend with the mechanical stability. For the parameters of Site GMGS3-W19, a change in S_h about 1 % is enough to destabilize the hydrate layer.

3.2 Ursa Basin, Northern Gulf of Mexico

Flemings et al. (2008) observed severe overpressure within $200\,\mathrm{m}$ below seafloor for sites U1322 and U1324 in the Ursa Basin in the Northern Gulf of Mexico, measured during Integrated Ocean Drilling Program (IODP) Expedition 308. The overpressure can reach 60 % of the hydrostatic effective stress $\sigma'_{vh} = \gamma'(H+D)$ for Site U1324 and 70 % for Site U1322. Take Site U1324 for an example, the pore pressure satisfies

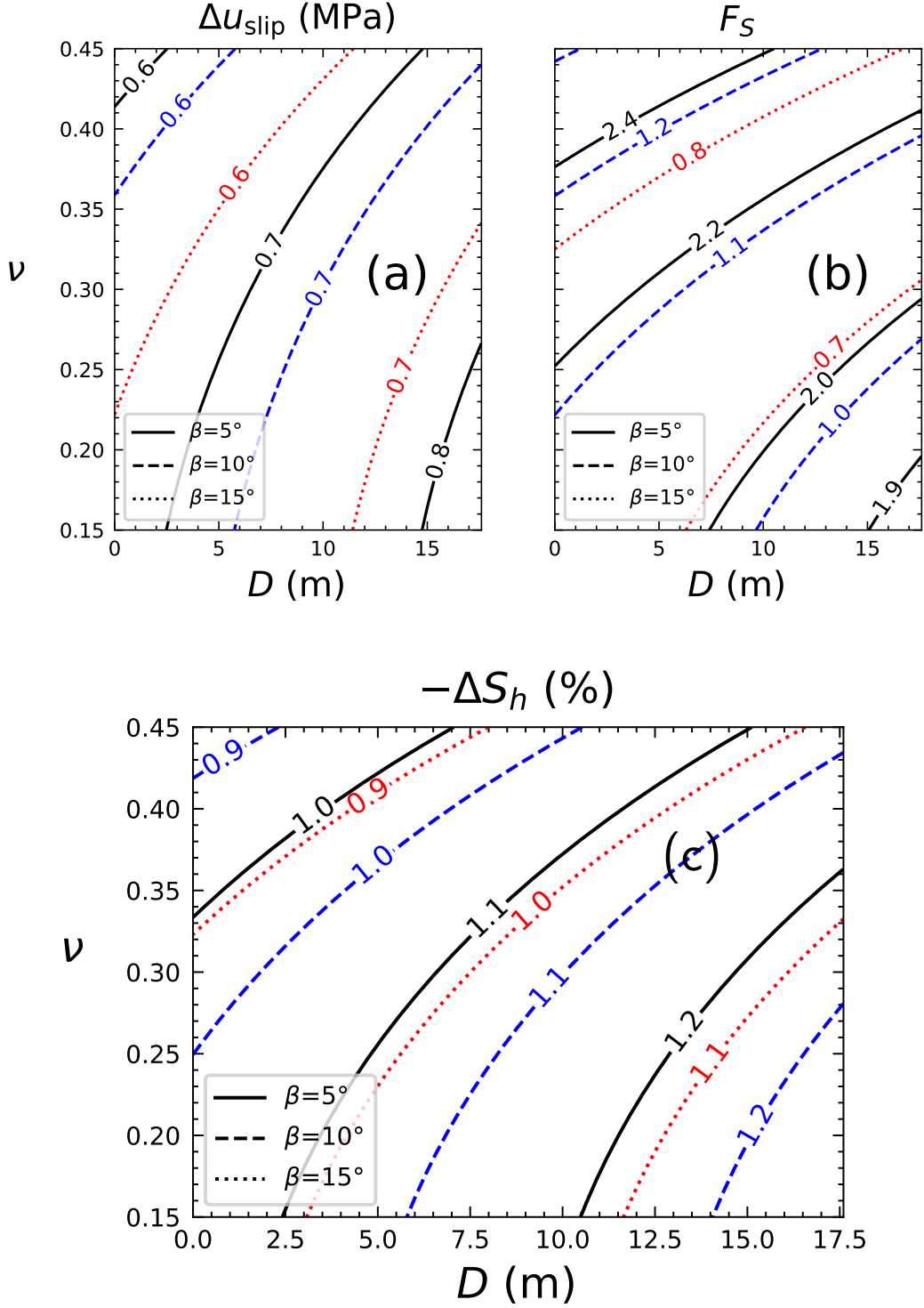$$\frac{\Delta u}{\gamma'(H+D)} = \lambda^* \approx 0.6, \tag{10}$$

Figure 3. Contour plots of (a) Δu_{slip} with variations in D and ν, (b) corresponding safety factor F_S, and (c) the amount of hydrate dissociated to generate Δu_{slip}. The styles of the contour lines denote the slope dip angle β. Smaller ν and β and thicker D all contribute to higher Δu_{slip}, and more hydrate must dissociate to initiate progressive failure. An amount of about 1 % is generally required. The solid, dotted and dashed contour lines are for the slope dip angles 5°, 10° and 15°, respectively. The corresponding F_S when progressive failure starts are mostly greater than unity, and for the small β case, F_S may even exceed 2.4, a value so high that in the infinite slope model no landslide should occur.

and with a slope dip angle $\beta = 2°$ and friction angle $\psi = 30°$, the safety factor is $F_S \geq$ 4.9, well above the critical value, which contrasts the fact that this site is prone to landslides. Infinite slope model allows limited options to reconcile this discrepancy: either a higher overpressure up to $0.93\sigma'_{vh}$ of the hydrostatic effective stress occurred during the Pleistocene at the time of the landslide, or the site then had a much steeper slope of 10°. Based on the geological evidence, neither explanation is well grounded.

A more straightforward explanation, however, is that the landslide is triggered by progressive failure. The failure onset occurs when

$$\gamma'(H + D)\left(\cos^2 \beta - \lambda^*\right) = \frac{\lambda_0 D_c G}{\Delta f a(1 - \nu)}. \tag{11}$$

Assuming a typical Poisson's ratio $\nu = 0.3$, Young's modulus $E \sim 10\,\text{MPa}$ and failure depth at $H + D \sim 200\,\text{m}$, the scaled rupture patch size where failure occurs is $\chi \approx 8.4$. For comparison, $\chi_{\min} \approx 3.4$ can be calculated using the parameters. The initial failure patch size $2a$ is notably only one order of magnitude larger than D_c.

4 Discussion

4.1 Effect of the scaled rupture size

The scaled rupture size $\chi = a/D_c$ is an important parameter in the slip nucleation model because it relates the asperity-scale frictional property D_c to the macroscopic rupture size a, but it is not well constrained. In modeling the site in Shenhu region we have used $\chi = 100$, and $\chi_{\min}$ can be calculated from eq. (6) to be around $35 - 50$ for the range of ν and β provided in Table 1, which is on the same order of magnitude as $\chi = 100$. Similarly, for the sites in Ursa Basin, $\chi_{\min} \approx 3.4$ is much smaller than that of the site in Shenhu region, and as a result, the scaled rupture size χ is accordingly reduced. Because Δu_{slip} can be expressed as

$$\Delta u_{\text{slip}} = \sigma_0(1 - \chi_{\min}/\chi), \tag{12}$$

a large χ requires a higher overpressure closer to σ_0. In this study we generally choose $\chi/\chi_{\min} \approx 2$, consistent with the treatment in Viesca and Rice (2012) for the scenario where the free surface is far from the sliding surface, i.e., $\sqrt{(H + D)/\chi_{\min} D_c} > 1$.

4.2 Note on the friction laws

We use the slip-weakening friction in the model because it is easy to derive the eigenvalue problem from the force balance. However, the result is not limited by the exact form of the friction laws as long as the friction drops as sliding, and we can also use the rate-weakening friction to derive similar results. For example, the Dieterich-Ruina friction constitutive law (Dieterich, 1979; Ruina, 1983) is

$$f = f_0 + A \ln \frac{V}{V_0} + B \ln \frac{V_0 \theta}{L}, \quad \frac{\mathrm{d}\theta}{\mathrm{d}t} = 1 - \frac{V\theta}{L} \tag{13}$$

where V is the sliding velocity, θ is a state variable representing the sliding history, L is a characteristic length scale, f_0 is the reference friction, V_0 is the reference velocity, and A and B are constants. Substitute the friction in eq. (3) and take the time derivative, we have

$$\left(A\frac{\dot{V}}{V} + B\frac{\dot{\theta}}{\theta}\right)(\sigma_0 - \Delta u) = -\frac{G}{2\pi(1 - \nu)} \int_{-a}^{a} \frac{\partial V(\xi, t)}{\partial \xi} \frac{\mathrm{d}\xi}{x - \xi}. \tag{14}$$

After scaling with V_{rms} and keeping only the leading order of V, the equation becomes the same as using the slip-weakening friction.

5 Conclusion

In this study, we have shown that the infinite slope model may overestimate the stability of submarine slopes, and the progressive failure model can be used to assess the risk of submarine landslides. The critical excess pore pressure required to initiate progressive failure is generally less than $1\,\text{MPa}$, and the corresponding amount of hydrate dissociated is $\sim 1\,\%$, which is much smaller than the critical pore pressure in the infinite slope model. On a potential failure surface deeper below the seafloor, with a gentler slope and more easily collapsing sediments, the overpressure required to initiate progressive failure is greater and the risk of landslides is lower. The critical excess pore pressure is also affected by the scaled rupture size $\chi = a/D_c$, which is not well constrained but is on the same order of magnitude with $\chi_{\min} = 0.579 G/\sigma_0 \Delta f(1-\nu)$. For some landslide sites where infinite slope analysis gives unrealistically high safety factors, the progressive failure model provides a more reasonable explanation.

6 Open Research

The python scripts of the model are available at `https://gitlab.com/jzchenjz/hydrate-induced-progressive-landslides`, open-sourced under MIT license.

Appendix A Landslide with slip-weakening friction

A1 Finite length rupture model

For a finite rupture patch located between $x = \pm a$ far from the free surface, follow the treatment of Viesca and Rice (2012) after scaling the spatial coordinates to place the rupture patch between $x = \pm 1$ we obtain

$$\frac{\Delta f a(1-\nu)}{D_c G}\left(\frac{\tau_0}{\tan\psi} - \Delta u\right)V = \frac{1}{2\pi}\int_{-1}^{+1}\frac{\partial V/\partial s}{x-s}\mathrm{d}s \tag{A1}$$

where V is $\mathrm{d}\delta/\mathrm{d}t$ scaled by its RMS value. At the boundaries of the rupture, $V(\pm 1) = 0$. The equation becomes an eigenvalue problem

$$\lambda V(x) = \frac{1}{2\pi}\int_{-1}^{1}\frac{V'(s)}{x-s}\mathrm{d}s, \tag{A2}$$

where the eigenvalue is

$$\lambda = \frac{\Delta f a(1-\nu)}{D_c G}\left(\frac{\tau_0}{\tan\psi} - \Delta u\right) \tag{A3}$$

and the smallest eigenvalue λ_0 corresponds to the nucleation of the rupture with minimum pore pressure increase. From eq. (A2) we can obtain

$$\lambda V(x) = -\frac{1}{2\pi}\int_{-1}^{1}V(y)\frac{\mathrm{d}}{\mathrm{d}y}\frac{1}{x-y}\mathrm{d}y, \tag{A4}$$

and with a uniform spacing $h = 1/N$, where $2N+1$ is the number of grid points on $[-1,1]$ we get

$$\lambda V(x_i) \approx -\frac{h}{2\pi}\sum_{j=-N}^{N}V(x_j)\left(\frac{\mathrm{d}}{\mathrm{d}y}\frac{1}{x_i-y}\right)\Bigg|_{y=x_j} = -\frac{1}{2\pi}\sum_{j=-N}^{N}V(x_j)\left(\frac{1}{x_i-x_{j+1/2}} - \frac{1}{x_i-x_{j-1/2}}\right)$$

$$= -\frac{h}{2\pi}\sum_{j=-N}^{N}\frac{V(x_j)}{\left(x_i-x_j\right)^2 - h^2/4} \tag{A5}$$

321 or with $V_i = V(x_i)$

$$\lambda V_i = -\frac{N}{2\pi} \sum_{j=-N}^{N} \frac{V_j}{(i-j)^2 - 1/4}, \tag{A6}$$

323 which can be written in a matrix form

$$\lambda V = KV \tag{A7}$$

325 where $V = (V_{-N}, V_{-N+1}, \ldots, V_{N-1}, V_N)^\intercal$ and K is a symmetric matrix

$$K_{ij} = -\frac{N}{2\pi[(i-j)^2 - 1/4]} \tag{A8}$$

327 with $2N+1$ real eigenvalues. The matrix is strictly diagonally dominant

$$|K_{ii}| > \sum_{j \neq i} |K_{ij}| \tag{A9}$$

329 and all diagonal elements are positive, so the eigenvalues are all positive by the Gersh-
330 gorin circle theorem. The smallest eigenvalue is $\lambda_0 \approx 0.579$. The excess pore pressure
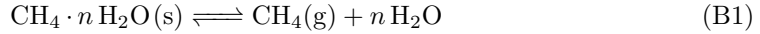331 is related to the crack length as

$$\Delta u_{\text{slip}} = \frac{\tau_0}{\tan\psi} - \frac{\lambda_0 D_c G}{\Delta f a (1-\nu)}. \tag{A10}$$

333 With an estimate of a/D_c, we can predict if the excess pore pressure Δu can cause a land-
334 slide.

Appendix B overpressurization due to hydrate dissociation

B1 Expansion factor

337   The density of methane hydrate is smaller than the density of water, so if there is
338 no gaseous phase released during hydrate dissociation (i.e., hydrate dissolution), no ex-
339 cess pore pressure is generated. With negligible methane solubility in the pore water,
340 with no gas phase present, the relative volume change to the pore volume in the reac-
341 tion

$$\mathrm{CH_4 \cdot n\,H_2O\,(s)} \rightleftharpoons \mathrm{CH_4(g)} + n\,\mathrm{H_2O} \tag{B1}$$

343 is

$$\frac{V_d}{V_p} = \frac{\Delta V_l + \Delta V_h + \Delta V_g}{V_p} = \frac{\Delta V_l + \Delta V_h + \Delta V_g}{\Delta V_h} \Delta S_h \tag{B2}$$

345 where V_d is the volume change during the dissociation assuming no pressure and tem-
346 perature change, V_p is the pore volume, ΔS_h is the change of pore volume hydrate frac-
347 tion, and subscripts w, h and g denote the pore water, the hydrates and the free methane
348 gas. The mass fraction of methane in the hydrate is treated as a constant x, close to 0.13
349 for an ideal hydration number $n = 5.75$, so the relations between the volume changes
350 are

$$\Delta V_g = -\frac{x\rho_h}{\rho_g}\Delta V_h, \quad \Delta V_l = -\frac{(1-x)\rho_h}{\rho_l}\Delta V_h \tag{B3}$$

352 and the total volume change relative to the pore volume V_p is $V_d/V_p = -R_v\Delta S_h$ where
353 the volume expansion factor R_v is

$$R_v = (1-x)\rho_h/\rho_l + x\rho_h/\rho_g - 1. \tag{B4}$$

355 The density of the hydrate can be treated as constant, and the pore water density can
356 be calculated using Spivey et al. (2004). The density of the methane gas is calculated
357 using an appropriate equation of state for methane, e.g., Setzmann and Wagner (1991).

In some works (e.g., Nixon & Grozic, 2007), R_v is simplified using $\rho_h/\rho_l \approx 1$ and the ideal gas approximation

$$R_v \approx \frac{x\rho_h}{\rho_g} - x = 164.6\frac{T_e}{T^{\ominus}}\frac{P^{\ominus}}{P} - 0.13 \tag{B5}$$

where T_e is the equilibrium temperature of the gas hydrate in Kelvin and P is the pressure in atm. The volume ratio 164.6 is calculated under a standard condition $P^{\ominus} = 1\,\text{atm}$ and $T^{\ominus} = 273.15\,\text{K}$.

B2 Total compressibility

We have calculated the volume expansion factor, which assumes constant temperature and pressure during the dissociation. However, the expanded volume is confined in the pore space. If the pores are taken as rigid, the additional liquid and gas must be compressed. The compressibility κ can be approximated in different means. For example, Nixon and Grozic (2007) used relations between the void ratio $e = \phi/(1-\phi)$, the effective stress σ', and empirically determined soil swelling index C_s. Xu and Germanovich (2006) avoided the empirical treatment using

$$\kappa = -\frac{1}{V}\frac{\mathrm{d}V}{\mathrm{d}P} = -\frac{1}{V}\left(\frac{\partial V}{\partial P} + \frac{\partial V}{\partial T_e}\frac{\mathrm{d}T_e}{\mathrm{d}P}\right) = \sum_i \frac{S_i}{\rho_i}\left(\frac{\partial \rho_i}{\partial P} + \frac{\partial \rho_i}{\partial T_e}\frac{\mathrm{d}T_e}{\mathrm{d}P}\right) = \kappa_g S_g + \kappa_l S_l \tag{B6}$$

where S_i is the saturation of the i-th component, ρ_i is the density of the i-th component, and T_e is the three-phase equilibrium temperature. The pressure and temperature dependence of the hydrate density is neglected, and the compressibility factors of the gas and liquid phases are

$$\kappa_g = \frac{1}{\rho_g}\left(\frac{\partial \rho_g}{\partial P} + \frac{T_e^2 R}{P\Delta H_m}\frac{\partial \rho_g}{\partial T_e}\right), \quad \kappa_l = \frac{1}{\rho_l}\left(\frac{\partial \rho_l}{\partial P} + \frac{T_e^2 R}{P\Delta H_m}\frac{\partial \rho_l}{\partial T_e}\right) \tag{B7}$$

where the Clapeyron-Clausius equation $\mathrm{d}T_e/\mathrm{d}P = T_e^2 R/(P\Delta H_m)$ is used, and $\Delta H_m = 54.44\,\text{kJ/mol}$ (Gupta et al., 2008) is the latent heat of methane hydrate dissociation. When calculating κ, we tested both Setzmann and Wagner (1991) and simpler Peng and Robinson (1976) models to calculate the methane gas density. The results are almost the same.

B3 Excess pore pressure in confined pores

In a confined pore of a volume V_p with saturation levels S_g, S_l, and $S_h = 1 - S_g - S_l$, when the hydrate saturation changes by $\mathrm{d}S_h$ and results in a pressure change $\mathrm{d}P$, the changes in S_g and S_l are

$$\mathrm{d}S_g = -\frac{\rho_h}{\rho_g}x\mathrm{d}S_h - \kappa_g S_g\mathrm{d}P, \quad \mathrm{d}S_l = -\frac{\rho_h}{\rho_l}(1-x)\mathrm{d}S_h - \kappa_l S_l\mathrm{d}P. \tag{B8}$$

Add the two equations and substitute $\mathrm{d}S_h = -\mathrm{d}S_g - \mathrm{d}S_l$, and we arrive at

$$\kappa\mathrm{d}P = -R_v\mathrm{d}S_h. \tag{B9}$$

The differential equations to solve are

$$\frac{\mathrm{d}P}{\mathrm{d}S_h} = -\frac{R_v}{\kappa} \tag{B10}$$

$$\frac{\mathrm{d}S_g}{\mathrm{d}S_h} = -\frac{\rho_h}{\rho_g}x - \kappa_g\frac{\mathrm{d}P}{\mathrm{d}S_h} \tag{B11}$$

During the dissociation, the pressure increases, so both R_v and κ are also changing. The equations are solved iteratively. Figure 2 shows the diagram of Δu with change of hydrate saturation and pressure.

Acknowledgments

References

Berndt, C., Costa, S., Canals, M., Camerlenghi, A., De Mol, B., Saunders, M., & Shearer, P. (2012, February 21). Repeated slope failure linked to fluid migration: The ana submarine landslide complex, eivissa channel, western mediterranean sea. *Earth Planet. Sci. Lett.*, *319-320*, 65–74. doi: 10.1016/j.epsl.2011.11.045

Brothers, D. S., Luttrell, K. M., & Chaytor, J. D. (2013, September). Sea-level–induced seismicity and submarine landslide occurrence. *Geology*, *41*(9), 979–982. doi: 10.1130/g34410.1

Brown, H. E., Holbrook, W. S., Hornbach, M. J., & Nealon, J. (2006, June). Slide structure and role of gas hydrate at the northern boundary of the storegga slide, offshore norway. *Mar. Geol.*, *229*(3-4), 179–186. doi: 10.1016/j.margeo.2006.03.011

Chen, J., Mei, S., Wang, D., Sun, J., & Sun, Y. (2023). https://gitlab.com/jzchenjz/hydrate-induced-progressive-landslides.

Dieterich, J. H. (1979). Modeling of rock friction .1. experimental results and constitutive equations. *J. Geophys. Res.*, *84*(Nb5), 2161–2168. doi: 10.1029/JB084iB05p02161

Duncan, J. M., Wright, S. G., & Brandon, T. L. (2014). *Soil strength and slope stability*. John Wiley & Sons, Inc.

Flemings, P., Long, H., Dugan, B., Germaine, J., John, C., Behrmann, J., & Sawyer, D. (2008, May). Pore pressure penetrometers document high overpressure near the seafloor where multiple submarine landslides have occurred on the continental slope, offshore louisiana, gulf of mexico. *Earth Planet. Sci. Lett.*, *269*(3-4), 309–325. doi: 10.1016/j.epsl.2007.12.005

Ginsburg, G. D., Soloviev, V. A., et al. (1995). Submarine gas hydrate estimation: theoretical and empirical approaches. In *Offshore technology conference.* doi: 10.4043/7693-ms

Gupta, A., Lachance, J., Sloan, E. D., & Koh, C. A. (2008, December). Measurements of methane hydrate heat of dissociation using high pressure differential scanning calorimetry. *Chem. Eng. Sci.*, *63*(24), 5848–5853. doi: 10.1016/j.ces.2008.09.002

Kayen, R. E., & Lee, H. J. (1991, January). Pleistocene slope instability of gas hydrate-laden sediment on the beaufort sea margin. *Mar. Geotechnol.*, *10*(1-2), 125–141. doi: 10.1080/10641199109379886

Koh, C. A., Sloan, E. D., Sum, A. K., & Wu, D. T. (2011, July). Fundamentals and applications of gas hydrates. *Annu. Rev. Chem. Biomol.*, *2*(1), 237–257. doi: 10.1146/annurev-chembioeng-061010-114152

Kvenvolden, K. A. (1988, December). Methane hydrate–a major reservoir of carbon in the shallow geosphere? *Chem. Geol.*, *71*(1-3), 41–51. doi: 10.1016/0009-2541(88)90104-0

Kwon, T.-H., Cho, G.-C., & Santamarina, J. C. (2008, March). Gas hydrate dissociation in sediments: Pressure-temperature evolution. *Geochem. Geophys. Geosyst.*, *9*(3), Q03019. doi: 10.1029/2007gc001920

Lafuerza, S., Sultan, N., Canals, M., Lastras, G., Cattaneo, A., Frigola, J., . . . Berndt, C. (2012, April). Failure mechanisms of ana slide from geotechnical evidence, eivissa channel, western mediterranean sea. *Mar. Geol.*, *307-310*, 1–21. doi: 10.1016/j.margeo.2012.02.010

Lee, J. Y., Santamarina, J. C., & Ruppel, C. (2010, March). Volume change asso-

ciated with formation and dissociation of hydrate in sediment. *Geochem. Geophys. Geosyst.*, *11*(3). doi: 10.1029/2009gc002667

Marone, C. (1998, May). Laboratory-derived friction laws and their application to seismic faulting. *Annu. Rev. Earth Planet. Sci.*, *26*(1), 643–696. doi: 10.1146/annurev.earth.26.1.643

Maslin, M., Owen, M., Betts, R., Day, S., Jones, T. D., & Ridgwell, A. (2010, April). Gas hydrates: past and future geohazard? *Philos. Trans. R. Soc. London, Ser. A*, *368*(1919), 2369–2393. doi: 10.1098/rsta.2010.0065

Nixon, M. F., & Grozic, J. L. H. (2007, March). Submarine slope failure due to gas hydrate dissociation: a preliminary quantification. *Can. Geotech. J.*, *44*(3), 314–325. doi: 10.1139/t06-121

Normandeau, A., MacKillop, K., Macquarrie, M., Richards, C., Bourgault, D., Campbell, D. C., . . . Clarke, J. H. (2021, June). Submarine landslides triggered by iceberg collision with the seafloor. *Nat. Geosci.*, *14*(8), 599–605. doi: 10.1038/s41561-021-00767-4

Peng, D.-Y., & Robinson, D. B. (1976, February). A new two-constant equation of state. *Ind. Eng. Chem. Fundam.*, *15*(1), 59–64. doi: 10.1021/i160057a011

Riboulot, V., Cattaneo, A., Sultan, N., Garziglia, S., Ker, S., Imbert, P., & Voisset, M. (2013, August). Sea-level change and free gas occurrence influencing a submarine landslide and pockmark formation and distribution in deepwater nigeria. *Earth Planet. Sci. Lett.*, *375*, 78–91. doi: 10.1016/j.epsl.2013.05.013

Rice, J. R., & Ruina, A. L. (1983, June). Stability of steady frictional slipping. *J. Appl. Mech.*, *50*(2), 343. doi: 10.1115/1.3167042

Ruina, A. (1983, December). Slip instability and state variable friction laws. *J. Geophys. Res.*, *88*(Nb12), 10359–10370. doi: 10.1029/jb088ib12p10359

Setzmann, U., & Wagner, W. (1991, November). A new equation of state and tables of thermodynamic properties for methane covering the range from the melting line to 625 k at pressures up to 100 MPa. *J. Phys. Chem. Ref. Data*, *20*(6), 1061–1155. doi: 10.1063/1.555898

Sloan, E. D., & Koh, C. (2007). *Clathrate hydrates of natural gases.* CRC press.

Smith, D., Harrison, S., & Jordan, J. (2013, December). Sea level rise and submarine mass failures on open continental margins. *Quat. Sci. Rev.*, *82*, 93–103. doi: 10.1016/j.quascirev.2013.10.012

Spivey, J. P., McCain, W. D., & North, R. (2004, July). Estimating density, formation volume factor, compressibility, methane solubility, and viscosity for oilfield brines at temperatures from 0 to 275 °c, pressures to 200 MPa, and salinities to 5.7 mole/kg. *J. Can. Pet. Technol.*, *43*(07). doi: 10.2118/04-07-05

Straus, J. M., & Schubert, G. (1977, January). Thermal convection of water in a porous medium: Effects of temperature- and pressure-dependent thermodynamic and transport properties. *J. Geophys. Res.*, *82*(2), 325–333. doi: 10.1029/jb082i002p00325

Sultan, N., Cochonat, P., Foucher, J.-P., & Mienert, J. (2004, December). Effect of gas hydrates melting on seafloor slope instability. *Mar. Geol.*, *213*(1-4), 379–401. doi: 10.1016/j.margeo.2004.10.015

Sun, J., Zhang, L., Ning, F., Lei, H., Liu, T., Hu, G., . . . Wu, N. (2017, September). Production potential and stability of hydrate-bearing sediments at the site GMGS3-w19 in the south china sea: A preliminary feasibility study. *Mar. Petrol. Geol.*, *86*, 447–473. doi: 10.1016/j.marpetgeo.2017.05.037

Viesca, R. C., & Rice, J. R. (2012, March). Nucleation of slip-weakening rupture instability in landslides by localized increase of pore pressure. *J. Geophys. Res. Solid Earth*, *117*(B3), 1–21. doi: 10.1029/2011JB008866

Wang, W., Wang, D., Wu, S., Völker, D., Zeng, H., Cai, G., & Li, Q. (2018, January). Submarine landslides on the north continental slope of the south china sea. *J. Ocean Univ. China*, *17*(1), 83–100. doi: 10.1007/s11802-018-3491-0

Xu, W., & Germanovich, L. N. (2006, January). Excess pore pressure resulting from

502   methane hydrate dissociation in marine sediments: A theoretical approach.   *J.*

503   *Geophys. Res.*, *111*(B1). doi: 10.1029/2004jb003600